Experimental Characterization of Transition Noise in HAMR

Kyungjin Kim and Jaekyun Moon

Department of Electrical Engineering Korea Advanced Institute of Science and Technology, Daejeon 305-701, Korea

Due to the sensitivity of the write process to temperature variations and laser position alignment, transition noise in heat-assisted magnetic recording (HAMR) may exhibit characteristics that are significantly different from those of conventional magnetic recording. In this work, statistical properties of transition noise in HAMR are investigated using real data taken off a spin stand. The Karhunen Loeve (K-L) expansion method is applied to the read waveforms corresponding to a pseudorandom bit pattern written at varying locations of a disk.

***Index Terms*—Karhunen-Loeve transforms, magnetic recording noise.**

I. Introduction

HEAT-ASSISTED magnetic recording (HAMR) is an emerging technology that can significantly increase the areal density of the current perpendicular magnetic recording (PMR) technology [1]. HAMR employs a high coercivity magnetic medium with very high anisotropy that allows retention of written magnetization patterns at reasonable temperatures despite the small magnetic grain sizes. To enable writing onto a high-coercivity medium, a naturally difficult task, HAMR utilizes a laser to locally heat the medium right before the writing magnetic pole flies above it. Heating temporarily reduces the coercivity of the medium, which enables the head field to switch the grains in the high-anisotropy medium. Due to the sensitivity of the write process to temperature variations and laser position alignments [1], [2], transition noise in HAMR may have significantly different characteristics compared to medium noise in conventional magnetic recording. It is important to have an accurate characterization of medium noise for a realistic channel model, which in turn is essential for developing reliable signal processing and coding schemes.

In this work, statistical properties of transition noise in HAMR are investigated using real data taken off a spin stand. The Karhune Loéve (K-L) expansion is a useful tool in decomposing a random process into orthogonal components whose coefficients are uncorrelated [6]. The K-L expansion technique has been used to investigate potentially different noise mechanisms of isolated magnetic transitions in [5]. We also employ the Karhune Loéve (K-L) expansion here, but we consider the noise waveforms corresponding to both isolated transitions and isolated pairs of consecutive transitions (“dibit” patterns) in hopes of constructing more realistic pattern-dependent noise models. Our goal is to extract orthogonal medium noise components and quantify their relative weights corresponding to a set of perpendicular HAMR spin-stand data. For comparison, PMR data taken from the same spin-stand are also analyzed using the same technique. The results indicate that for isolated transitions in PMR, the position jitter component accounts for about 80% of the total noise power whereas the width fluctuation component takes up 9–13%. This appears consistent with the results reported in [3]. For the HAMR case, however, our results show that for isolated transitions, the position jitter and width fluctuation components account for approximately 60% and 30%, respectively, pointing to a more pronounced width variation effect relative to conventional PMR. We surmise that the sensitivity of the half-height width (PW50) of the read pulse to temperature fluctuations and accuracy of laser position alignment [2]. They contribute to the relatively high width-variation component in the isolated transitions of HAMR.

For isolated dibits, the dominant noise mode appears to be the one corresponding to amplitude fluctuation, which may be related to partial erasure of closely-spaced transitions and/or transition position shifts that are negatively correlated (i.e., two transitions either pulling or pushing each other). The second significant effect associated with the dibits may be explained by positively-correlated position shifts (i.e., two transitions shifting in the same direction).

Finally, a procedure for constructing a simple model for pattern-dependent media noise is presented. The model assumes that the given pattern consists of only isolated transitions and isolated dibits, which would be a reasonable scenario for written bit sequences coded by the maximum-transition-run (MTR) code with a constraint $j = 2$ [8].

II. Analysis of Experimental Data

A. Measurement

The HAMR system under study employs a FePtL10 thin-film disk and a shielded pole head designed for PMR systems. In order to analyze the statistical properties of the read signal, a 127-bit pseudo-random pattern is written in several locations of the disk. Repeated read passes are then taken over the written data. These multiple read passes are then time-interpolated, aligned to minimize the squared error and then averaged to remove any data-independent noise. Although not shown here, the autocorrelation of the removed noise exhibits the typical stationary characteristic as well the sharp-correlation behavior of the additive system noise.

After the system noise is removed, the waveform corresponding to different locations are again time-aligned with one

Manuscript received November 05, 2012; revised January 07, 2013; accepted January 15, 2013. Date of current version July 15, 2013. Corresponding author: K. Kim (e-mail: happykkj@kaist.ac.kr).

Color versions of one or more of the figures in this paper are available online at http://ieeexplore.ieee.org.

Digital Object Identifier 10.1109/TMAG.2013.2242867

another in the sense of squared-error minimization. Let $s^{(i)}(t)$ be the resulting time-aligned read waveform corresponding to the pseudo-random bit-pattern written at the i-th location. The fluctuations seen across different $s^{(i)}(t)$'s can be safely assumed to reflect medium noise. The autocovariance function of the medium noise can be estimated from:

$$K_m(t_1,t_2) \cong \frac{1}{L}\sum_{i=1}^{L} m^{(i)}(t_1)m^{(i)}(t_2) \quad (1)$$

where $m^{(i)}(t) = s^{(i)}(t) - s^{av}(t)$ with $s^{av}(t) = (1/L)\sum_{i=1}^{L} s^{(i)}(t)$. In our experiment, $L = 34$.

B. Karhunen Loéve Expansion

The K-L expansion technique has been used to decompose transition noise into orthogonal directions corresponding to position jitter and width fluctuations [5]. The work of [5] focuses on isolated transitions. Here we use the technique on both isolated transitions and isolated dibits in an effort to construct a pattern-dependent noise mode. For some random process $m(t)$, the K-L expansion is defined [6] as

$$m(t) = \sum_{k=1}^{\infty} m_k\phi_k(t) \quad (m.s.) \quad (2)$$

with

$$m_k \triangleq \int_{[a,b]} m(t)\phi_k^*(t)dt \quad (3)$$

where the orthonormal basis functions $\phi_k(t)$ are the eigenfunctions of the autocovariance function $K_m(t_1,t_2)$ of $m(t)$, i.e.,

$$\int_{[a,b]} K_m(t_1,t_2)\phi_k(t_2)dt_2 = \lambda_k\phi_k(t_1) \quad (4)$$

with λ_k's denoting the corresponding eigenvalues. The coefficients m_k's in (2) are statistically independent of one another. The equality of (2) is in the sense of mean-squared error, i.e., the mean-squared error between the two sides of the equality approaches zero as the number of terms in the summation grows to infinity. The interval $[a,b]$ of integration corresponds to the observation interval for $m(t)$. By Mercer's theorem [6], we can also write

$$K_m(t_1,t_2) = \sum_{k=1}^{\infty} \lambda_k\phi_k(t_1)\phi_k^*(t_2). \quad (5)$$

The eigenvalues represent variances of the noise components in each orthogonal direction: $\lambda_k = E\{m_k^2\}$.

In applying the K-L expansion method, we first estimate the autocorrelation functions of the medium noise at locations within the 127-bit pseudo-random pattern corresponding to isolated transitions.

For each location, the eigenfunctions and the corresponding eigenvalues are extracted by numerically solving the integral equation of (3). To accurately locate isolated transition positions from the read waveform in the presence of potential signal interference from neighboring (albeit well-separated) transitions, an isolated transition response was first constructed by numerically searching for a step response that would give rise to the observed read waveforms in sparse transition density regions (to avoid any potential nonlinear distortions). This isolated transition response was then used to construct a linearly-superimposed, clean read waveform corresponding to the given pseudo-random pattern. This linearly-constructed waveform can be compared with the averaged waveform to locate the exact positions of the isolated transitions. Table I shows the extracted eigenvalues for isolated transitions for both the HAMR and PMR measurements. Identical steps were taken to analyze data from a PMR system. The same head was used along with a CoCrPt alloy thin-film disk for the PMR measurements. Each eigenvalue, which represents the power of the noise component along the corresponding orthogonal direction, is shown as a percentage of the total sum. Two largest eigenvalues make up for the most of the noise power. The results appear consistent among all four isolated transitions found in the 127-bit pattern. Note that the isolated transitions are shown in the middle of the given local bit patterns. As can be seen, the isolated transitions are separated from another transitions by at least two zeros on either side. The corresponding two most significant eigenfunctions are shown in Fig. 1. The shapes suggest that the first eigenfunction may correspond to position jitter in that it gives a fairly good match to the first-order derivative of the transition response. Likewise, the second eigenfunction may be associated with the width fluctuation as it provides a reasonable match against the first-order derivative of $h(t)$ with respect to its width parameter.

TABLE I
COMPARISON OF EIGENVALUES FOR ISOLATED TRANSITIONS IN HAMR AND PMR

local data pattern											HAMR		PMR	
											$\lambda_1(\%)$	$\lambda_2(\%)$	$\lambda_1(\%)$	$\lambda_2(\%)$
0	-1	0	0	0	1	0	0	0	0	0	65.4	30.3	79.6	13.1
0	0	0	0	0	-1	0	0	0	1	0	65.5	30.0	81.2	8.8
-1	0	0	0	0	1	0	0	-1	1	0	65.2	30.1	80.9	10.2
0	-1	1	0	0	-1	0	0	1	0	0	65.2	30.5	80.7	8.9

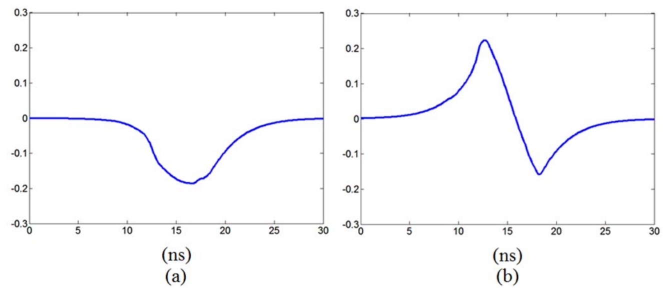

Fig. 1. First (a) and second (b) eigenfunctions associated with isolated transitions in HAMR.

In fact, expressing the local transition noise associated with a single transition using the first-order Taylor series approximation involving random position jitters and width variations [4] gives

$$m(t) \cong \triangle j\frac{\partial h(t)}{\partial t} + \triangle w\frac{\partial h(t)}{\partial w} \quad (6)$$

TABLE II
COMPARISON OF EIGENVALUES FOR ISOLATED DIBITS IN HAMR AND PMR

local data pattern										HAMR		PMR	
										$\lambda_1(\%)$	$\lambda_2(\%)$	$\lambda_1(\%)$	$\lambda_2(\%)$
0	0	0	0	1	-1	0	0	1	-1	78.7	13.8	70.1	22.7
0	1	0	0	-1	1	0	0	0	-1	72.3	19.1	60.1	33.7

where $h(t)$ is the transition response positioned at $t = 0$, and $\triangle j$ and $\triangle w$ represent the deviations of transition position and width, respectively, around some nominal values. Although $h(t)$ is expressed as a function only of t, it is implied that it depends also on the width parameter w. Note that it can be shown that $(\partial h(t)/\partial t)$ and $(\partial h(t)/\partial w)$ are orthogonal for typical transition responses. Comparing this with (2), we can also write

$$m(t) \cong m_1\phi_1(t) + m_2\phi_2(t) \quad (m.s.) \tag{7}$$

with

$$\triangle j = c_1 m_1 = c_1 \int_{[a,b]} m(t)\phi_1(t)dt \tag{8}$$

$$\triangle w = c_2 m_2 = c_2 \int_{[a,b]} m(t)\phi_2(t)dt \tag{9}$$

provided

$$\phi_1(t) = c_1 \frac{\partial h(t)}{\partial t}, \quad \phi_2(t) = c_2 \frac{\partial h(t)}{\partial w} \tag{10}$$

where c_1 and c_2 are normalization constants. In practice, neither $(\partial h(t))/(\partial t)$ is exactly a scaled version of $\phi_1(t)$, nor the shape of $(\partial h(t)/\partial w)$ gives a precise match to that of $\phi_2(t)$. In our numerical analysis, c_1 and c_2 are found such that the energy differences between $\phi_1(t)$ and $c_1(\partial h(t))/(\partial t)$ and between $\phi_2(t)$ and $c_2(\partial h(t))/(\partial w)$ are minimized.

Table I indicates that like in PMR, transition noise in HAMR can be mostly accounted for by position jitter and width fluctuation components. As in PMR, the jitter component (λ_1) is bigger but the relative strength of the width component (λ_2) is more visible in HAMR than in PMR. The sensitivity of PW50 with respect to variations in temperature and laser alignment is well-known [1], [2]. The significant width variation component of HAMR in Table I is consistent with this observation. The samples of $c_k m_k$ for $k = 1, 2$ (corresponding to those of $\triangle j$ and $\triangle w$, respectively) are obtained from each isolated transition location of each medium noise sample waveform utilizing (8) and (9). Fig. 3 shows the histograms of the sample values for $\triangle j$ and $\triangle w$ for both HAMR and PMR systems. The sample values are given in units of nanosecond (ns). As a reference, the minimum transition spacing T is 2.1 ns, and for the given head-medium speed, this corresponds to 27.43 nanometer (nm).

The same K-L expansion analysis is applied to the segments of the noise waveforms corresponding to the locations where dibits are written. Fig. 2 shows the two dominant eigenfunctions, the shapes of which look similar to those of the isolated transitions. Given the nominal read signal shape associated with a dibit, though, the eigenfunctions of Fig. 2 represent different basis functions. Namely, the one shown in Fig. 2(a) is best described as the amplitude fluctuation component whereas the shape in Fig. 2(b) can be attributed to shifts of both transitions moving in the same direction. The first eigenfunction seemingly associated with dibit amplitude fluctuation may come from the well-known nonlinear partial erasure effect [7] and/or negatively-correlated position shifts (i.e., two transitions within the dibit moving in the opposite directions). Again, the first two eigenvalues make up for more than 90 % of the sum. It can be seen that the dibits are isolated by at least two zeros on either side.

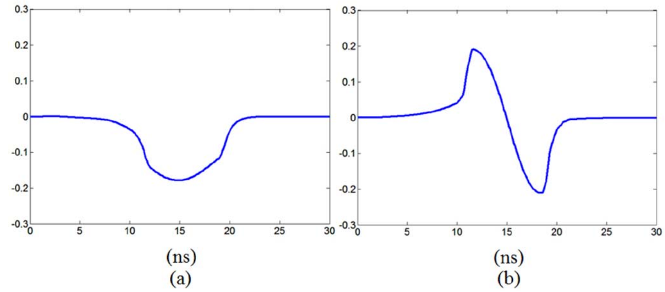

Fig. 2. First (a) and second (b) eigenfunctions associated with isolated dibits in HAMR.

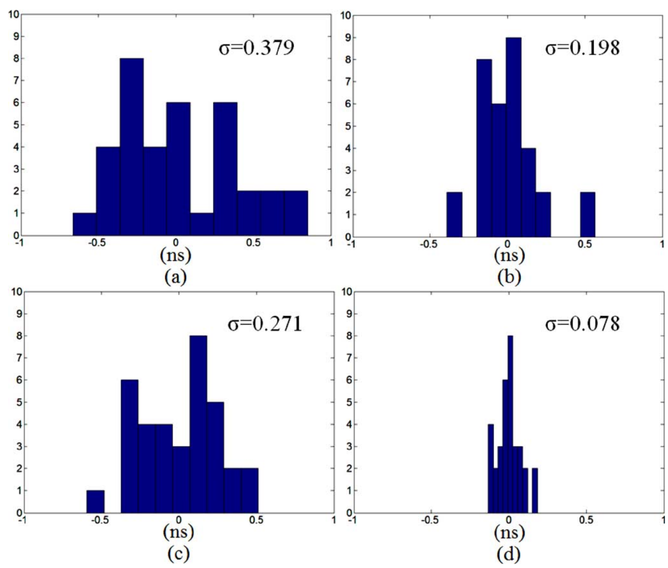

Fig. 3. Histograms of jitter and width sample values. (a) jitter for HAMR; (b) jitter for PMR; (c) width for HAMR; (d) width for PMR.

III. APPLICATION TO CHANNEL MODELING

Given the results of the K-L analysis we show how we can construct a channel model with pattern-dependent noise. Since we have noise characterization for isolated transitions and dibits only, we focus on the written data subject to the MTR code constraint that allows only up to two consecutive transitions to be written in the medium [8].

The goal here is to create a channel output model (a read signal and noise model) for an MTR-coded arbitrary data pattern. The basic strategy is to scan the given data with a fixed window that spans four bit intervals. By looking at the local transition pattern captured within the moving window, we add

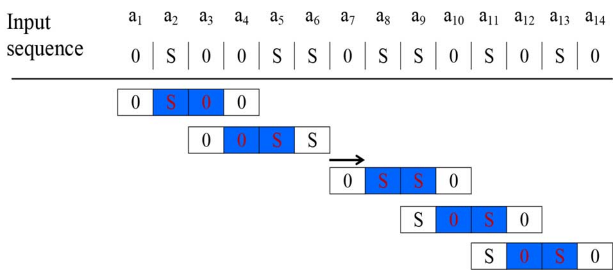

Fig. 4. Constructing a local-pattern-dependent noise model.

appropriate medium noise to the signal. The basic signal and noise model is

$$r(t) = \sum_{k} \{a_k h(t - kT) + m_k(t)\} + n(t). \tag{11}$$

where a_k represents the polarity of the transitions, T is the bit interval (minimum transition spacing), $m_k(t)$ is the local medium noise and $n(t)$ is the additive system noise.

Whenever there is a single transition, we add the medium noise component after appropriate alignment according to:

$$m_k(t) = \triangle j_k \phi_1(t - kT) + \triangle w_k \phi_2(t - kT). \tag{12}$$

The individual jitter and width values, $\triangle j_k$ and $\triangle w_k$, can be generated by random number generators with pre-specified variance values and distribution type (e.g., Gaussian). When there is a dibit captured within the window, we similarly align and add appropriate medium noise components. The difference is that the two basis functions of (12) are now replaced by those corresponding to the amplitude fluctuation and unison-jitter components shown in Fig. 2. Also, note that the noise waveform now should span two consecutive intervals. Again, the amplitude fluctuation and unison-jitter sample values can be generated by random number generators with pre-specified variance values and distribution type.

Fig. 4 illustrates this process. Here, S signifies the presence of a magnetic step or transition and "0" means no transition. As seen in the example, when the window of width four captures "S 0" in the middle, noise waveform for the isolated transition is added and the window moves to the right by two positions. If it captures "0 S" in the middle, the right most slot of the window will have either "S" or "0". If the latter is the case, then again noise corresponding to the isolated single transition is added. If there is "S" in the right-most slot, on the other hand, the noise waveform corresponding to the isolated dibit is written (for the two intervals corresponding to bit positions 5 and 6 in this example). Now the window jumps by four positions and the process repeats. If the captured pattern in the middle is "S S" as seen in the example, then simply add the noise waveform corresponding to the dibit and shift the window by two positions. The only remaining possibility is to see "0 0" in the middle of the window, which obviously means that no medium noise should be added. So, the window moves normally by two positions at a time, except when "0 S S" is encountered in the three right slots of the window at which time the next window position jumps by four. In summary, in constructing a readback waveform with proper medium noise components, local pattern-dependent noise waveforms can be added in a sequential fashion as the given data sequence is scanned serially.

IV. Conclusion

Experimentally captured data from a perpendicular HAMR spin stand have been analyzed using the K-L expansion technique. Specifically, we applied the noise decomposition method to isolated transitions and isolated dibit transition pairs within a pseudo-random pattern. The results suggest strong transition jitter and width fluctuation components in isolated transitions with jitter being the stronger component. Compared to a conventional PMR system, however, the width component is more visible. In the dibit region, the medium noise appears to have a dominating amplitude fluctuation component with some positively-correlated jitter component. Finally, a procedure has been established for constructing a pattern-dependent medium noise model for MTR-coded data consisting only of isolated transitions and isolated dibits.

Acknowledgment

This work was supported by the National Research Foundation of Korea under Grant 2012-0008719.

References

[1] M. Kryder *et al.*, "Heat assisted magnetic recording," in *Proc. IEEE*, Nov. 2008, vol. 96, no. 11.
[2] T. Rausch, J. A. Bain, D. D. Stancil, and T. E. Schlesinger, "Thermal Williams—Comstock model for predicting transition lengths in a heat assisted magnetic recording system," *IEEE Trans. Magn.*, vol. 40, no. 1, pp. 137–147, Jan. 2004.
[3] C. Fu, Z. Jin, H. N. Bertram, Y. Wu, and D. Guarisco, "Measurements and analysis of transition noise in perpendicular media," *IEEE Trans. Magn.*, vol. 39, no. 5, Sept. 2003.
[4] J. Moon, L. R. Carley, and R. R. Katti, "Density dependence of noise in thin metallic longitudinal media," *J. Appl. Phys.*, vol. 63, no. 8, Apr. 1988.
[5] S. W. Yuan and H. N. Bertram, "Statistical data analysis of magnetic recording noise mechanisms," *IEEE Trans. Magn.*, vol. 28, no. 1, Jan. 1992.
[6] H. Stark and J. W. Woods, *Probability, Statistics, and Random Processes for Engineers*, 4th ed. U.K.: Pearson, 2012.
[7] C. M. Melas, P. C. Arnett, I. A. Beardeley, and D. Palmer, "Nonlinear superposition in saturation recording," *IEEE Trans. Magn.*, vol. 23, no. 5, Sep. 1987.
[8] J. Moon and B. Brickner, "Maximum transition run codes for data storage systems," *IEEE Trans. Magn.*, vol. 32, no. 5, Sep. 1996.